[4] Santeler, D. J., "Outgassing Characteristics of Various Materials," *Transactions of Fifth National Symposium on Vacuum Technology*, Pergamon Press, New York, 1968, pp. 1–8.
[5] Barrer, R. M., *Diffusion in and through Solids*, Chaps. 9 and 10, Cambridge University Press, Cambridge, Mass., 1951.
[6] Dayton, B. B., "Relations between Size of Vacuum Chamber, Outgassing Rate and Required Pumping Speed," *Transactions of the Sixth National Symposium on Vacuum Technology*, Pergamon Press, New York, 1959, pp. 101–119.

Predicted Effects of Motor Parameters on Solid Propellant Extinguishment

R. L. Coates* and M. D. Horton*
Brigham Young University, Provo, Utah

Nomenclature

A = nozzle area
B = constant
c = heat capacity
C^* = characteristic velocity
E = activation energy
K_n = (burning area)/(throat area)
k = thermal conductivity
L^* = (chamber volume)/(throat area)
n = burning rate exponent = $d(\ln\bar{r})/d(\ln\bar{p})$
p = pressure
r = burning rate
T = temperature
x = distance
α = thermal diffusivity
γ = ratio of specific heats
ρ = density
$(\bar{\ })$ = bar denotes initial steady state

Subscripts

c = chamber average
f = flame, final value
g = gas
i = initial value
p = value at p
s = surface, solid
∞ = far beneath surface

Introduction

THEORETICAL studies[1–4] have shown that burning solid propellants can be extinguished by rapidly reducing the pressure in the combustion chamber. Early experimental studies[5] showed that if the depressurization process were characterized by either $t_{1/2}$, the time required to reduce the pressure to one-half of the initial steady-state value, or the corresponding average depressurization rate during the time $t_{1/2}$, a reproducible marginal extinguishment condition could be measured. Extinguishment will occur if $t_{1/2}$ is less than some critical value. The models of extinguishment also predict this behavior.

Much of the experimental study of extinguishment by rapid depressurization has been devoted to studying the effect of propellant composition on $t_{1/2}$.[1,6–8] In addition, the effects of initial pressure and ambient pressure have been investigated. The most recent studies[4,8] have shown that motor configuration can have an important effect. This Note presents the results of further theoretical investigation of the effect of motor configuration, in particular the effect of varying the L^* of the motor.

Received June 2, 1970; presented as Paper 70-664 at the AIAA 6th Propulsion Joint Conference, San Diego, Calif., June 15–19, 1970; revision received August 26, 1970. Work supported by AFOSR Grant AF-AFOSR-0897-67 and AFRPL Contract F04611-69-C-0045.

* Associate Professor, Chemical Engineering Department.

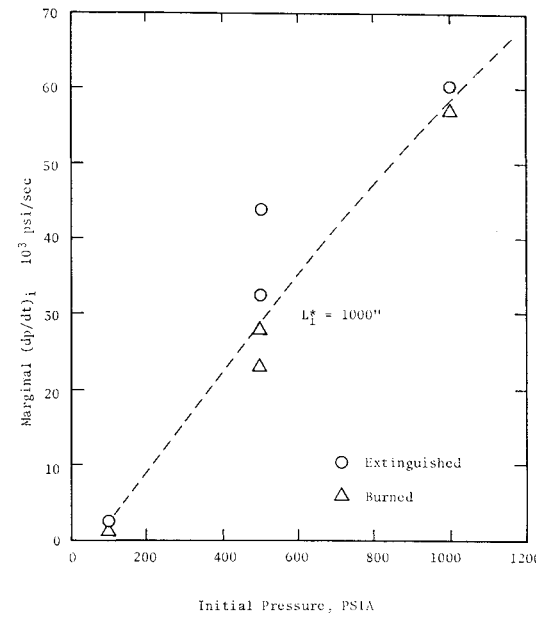

Fig. 1 Predicted effect of varying initial pressure.

Theory

The transient combustion process leading to extinguishment is assumed to be represented by a one-dimensional temperature profile, with a planar boundary separating the unburned solid and the combustion gases.[4] The solid is divided into finite-difference elements, and the following energy balance, taken on an element of the solid, is assumed to describe the transient heat conduction beneath the burning surface:

$$\frac{dT_i}{dT} = \alpha \frac{T_{i-1} - 2T_i + T_{i+1}}{(\Delta x)^2} + r \frac{T_{i+1} - T_{i-1}}{2\Delta x} \qquad (1)$$

The simplified combustion theory of Denison and Baum[9] is followed to compute the heat flux to the solid. The flux is related to the burning rate, surface temperature, and flame

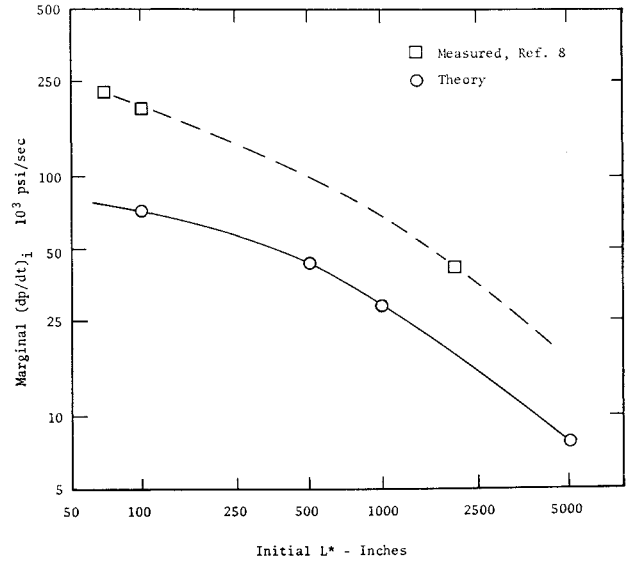

Fig. 2 Predicted effect of varying initial L^*; recent experimental data are also shown for comparison.

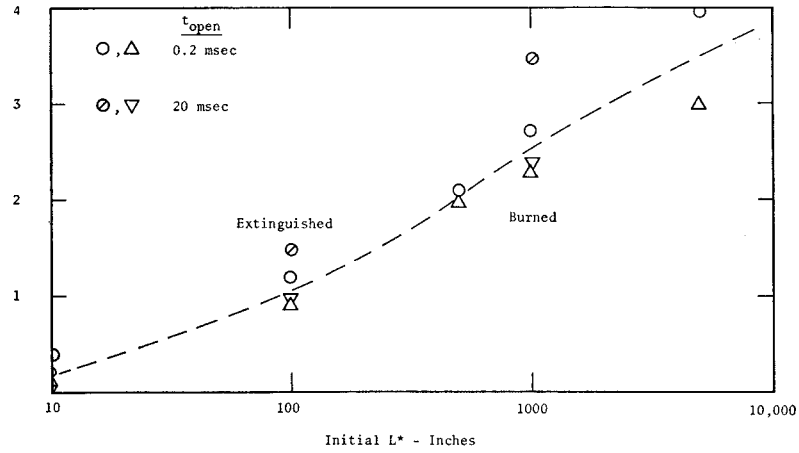

Fig. 3 Predicted effect of varying nozzle opening time.

temperature according to the following equations:

$$(-k\,dT/dx)_{x=0+} = r\rho_s[c_s(T_s - T_\infty) + c_g(\bar{T}_f - T_f)] = (T_0 - T_2)/2\Delta x \quad (2)$$

$$r = \bar{r}_p \exp[(-E_s/R)(1/T_s - 1/\bar{T}_{s,p})] \quad (3)$$

$$r = \bar{r}_p(T_f/\bar{T}_{f,f})^{n+1} \exp[-(E_f/R)(1/T_f - 1/\bar{T}_{f,p})] \quad (4)$$

The effect of the instantaneous pressure is manifested in these equations through $\bar{r}_p$, the steady-state burning rate that corresponds to a steady-state pressure equal to the instantaneous pressure p. This is a departure from the original theory, which has the benefit of forcing the theory to conform to experimental data for steady-state burning. Thus, the transient rates are computed by applying a correction to the empirical steady-state data, the correction factor depending upon the temperature distribution throughout the combustion wave.

This model for the solid propellant combustion process has been combined with equations describing the transient ballistics of a solid rocket motor. Equations expressing conservation of mass and energy inside the motor[10] are used in the following forms in the present study:

$$dp/dt = \gamma(\bar{p}/\tau_c)(T_c/\bar{T}_c)[(T_f/T_c)r/\bar{r} - W_n] \quad (5)$$

$$dT_c/dt = (T_c/p)\,dp/dt - (T_c/\tau_c)(\bar{p}/p)(T_c/\bar{T}_c)(r/\bar{r} - W_n) \quad (6)$$

where

$$\tau_c = \tilde{L}^*/C^*\gamma[2/(\gamma+1)]^{(\gamma+1)/(\gamma-1)} \quad (7)$$

$$W_n = (\bar{T}_c/T_c)^{1/2}(p/\bar{p})(A/A) \quad (8)$$

Prediction of $p(t)$ requires the simultaneous numerical integration of these equations along with those presented above for the solid burning rate. This was accomplished employing a numerical integration scheme based on Adams method.[11] Computations are made using a Librascope L-3055 computer.

Table 1 Properties of model propellant

Burning rate @ 1000 psia, in./sec	0.4
Exponent @ 1000 psia	0.4
Flame temperature, °K	3000
Surface temperature @ 1000 psia, °C	600
Solid density, lb/in.^{3}	0.060
γ	1.2
C^*, ft/sec	4800
$(c_p)_s/(c_p)_g$	0.5
α, in.^{2}/sec	0.00025
T_∞, °C	25
$E_s = E_g$, kcal/mole	20

Results of Parametric Calculations

Before studying the effect of L^* variation, calculations were made to verify that the theory predicts the same effect of p_i that is commonly observed. Model propellant properties were assumed as listed in Table 1. To represent the steady-state effect of pressure on a typical propellant, the following Summerfield burning rate law and corresponding K_n law were assumed:

$$p/r = 250 + 22.5\,p^{2/3} \quad (9)$$

$$K_n = 0.112\,p/r \quad (10)$$

where p is in psia and r is in in./sec.

In the computation procedure the input variables that govern the depressurization transient, in addition to the propellant properties, are the burning-area/throat-area ratio K_n, the initial L^*, the initial-nozzle-area/final-nozzle-area ratio, and the ambient pressure (assumed herein to be 1 psia). For the first calculations, the L_i^* and the opening time were held constant at 500 in. and 0.2 msec, respectively; p_i's of 100, 500, and 1000 psia were selected; and $A/\bar{A}$ was varied systematically until the marginal depressurization rate for extinguishment was located. Results of these calculations

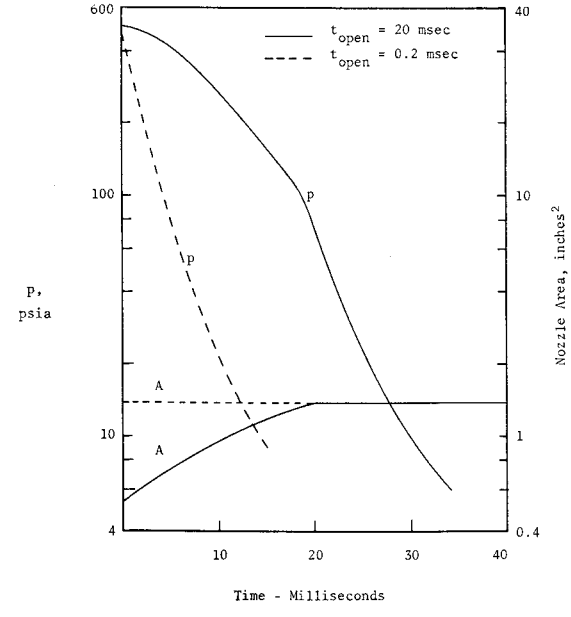

Fig. 4 Predicted transients showing the effect of nozzle opening time; the final/initial nozzle area ratio for these runs is 2.53; the marginal ratio for extinguishment is 2.1.

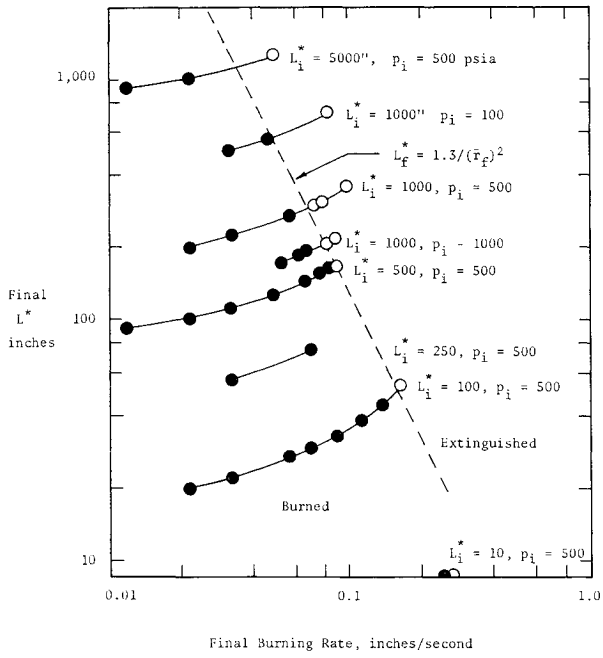

Fig. 5 Correlation of predicted termination transients; the data are plotted without regard for variations in dp/dt.

(Fig. 1) show that the marginal $(dp/dt)_i$ increases as p_i increases, in accordance with customary experimental observations.

In the second set of calculations L_i^* was varied from 100 in. to 5000 in. for p_i = 500 psia (K_n = 186.3) and an opening time of 0.2 msec. The marginal $(dp/dt)_i$ was predicted to be reduced from 70,000 psi/sec to less than 10,000 psi/sec as L^* was increased from 100 in. to 5000 in. (Fig. 2). Experimental data extracted from Ref. 8 show this same trend (Fig. 2).

In the next set of calculations the nozzle opening time was increased to 20 msec; the surprising result was that the marginal over all nozzle-area change was affected very little (Fig. 3). Figure 4 shows that the predicted effect of the greater opening time is to decrease dp/dt by approximately a factor of four until p reaches 100 psia. At this p, which corresponds to a time just prior to the nozzle being completely open, the $d(\ln p)/dt$ for the slowly opened case suddenly increases to near that of the rapidly opened case. This rapid change is apparently due to transient burning rate effects. For both cases illustrated, the nozzle-area ratio is near the marginal ratio below which extinguishment does not occur. Thus the important point illustrated by this figure is that the initial depressurization rate does not distinguish marginal extinguishment conditions in this case and, therefore, appears to have little value to the designer.

After several attempts using different approaches, it was discovered that all of the results of this parametric study could be correlated in terms of the motor L^* following opening of the nozzle L^*_f, and the burning rate $\bar{r}_f$ that would result from the nozzle-area change provided steady-state ballistics apply. Figure 5 presents all of the data plotted this way. The line $L^*_f = 1.3/\bar{r}^2$ provides a reasonable correlation of the marginal extinguishment conditions.

References

[1] Horton, M. D., Bruno, P. S., and Graesser, E. C., "Depressurization Induced Extinction of Burning Solid Propellants," *AIAA Journal*, Vol. 6, No. 2, Feb. 1968, pp. 292–297.

[2] Wooldridge, C. E., Marximan, G. A., and Kier, R. J., "A Theoretical and Experimental Study of Propellant Combustion Phenomena during Rapid Depressurization," Final Report, Contract NAS 1-7349, Feb. 1969, Stanford Research Institute, Menlo Park, Calif.

[3] Merkle, C. L., Turk, S. L., and Summerfield, M., "Extinguishment of Solid Propellants by Rapid Depressurization: Effects of Propellant Parameters," AIAA Paper 69-176, New York, 1969.

[4] Coates, R. L. and Horton, M. D., "Prediction of Conditions Leading to Extinguishment," *Proceedings of 6th ICRPG Combustion Conference*, CPIA Publications 192, Vol. 1, Dec. 1969, Silver Spring, Md., pp. 399–409.

[5] Ciepluch, C. C., "Effect of Rapid Pressure Decay on Solid Propellant Combustion," *ARS Journal*, Vol. 31, 1961, pp. 1584–1586.

[6] Ciepluch, C. C., "Effect of Composition on Combustion of Solid Propellants Using a Rapid Pressure Decrease," TN D-1559, 1962, NASA.

[7] "A Stop Start Study of Solid Propellants," Final Report, Contract NAS 1-6601, Nov. 1967, United Technology Center, Sunnyvale, Calif.

[8] "An Experimental Study of Solid Propellant Extinguishment by Rapid Depressurization," Preliminary Final Report, Contract NAS 1-7815, 1969, United Technology Center, Sunnyvale, Calif.

[9] Denison, M. R., and Baum, E., "A Simplified Model of Unstable Burning in Solid Propellants," *ARS Journal*, Vol. 31, No. 8, Aug. 1961, pp. 1112–1122.

[10] Coates, R. L., Polzien, R. E., and Price, C. F., "Design Procedures for Combustion Termination by Nozzle Area Variation," *Journal of Spacecraft and Rockets*, Vol. 3, No. 3, March 1966, pp. 418–425.

[11] Conte, S. D., *Elementary Numerical Analysis*, McGraw-Hill, New York, 1965, pp. 234–238.

Dynamic Response of Hydraulic Hoses

G. M. SWISHER*
Wright State University, Dayton, Ohio
AND
E. O. DOEBELIN†
Ohio State University, Columbus, Ohio

THE effects of hydraulic line dynamics on the over-all performance of a hydraulic control system were reported earlier.[1] Distributed-parameter and lumped-parameter models of metal lines were compared. This Note addresses the effects when braided hydraulic hoses, which expand when pressurized, are used. No investigators have reported on the degrading effect on dynamic response that occurs when hydraulic hoses are used in control systems.

The system studied was a closed-loop electrohydraulic position servo consisting of 1) a hydraulic cylinder as the power device; 2) two linear variable differential transformers (LVDT's) as the feedback and measurement elements; 3) an electronic servoamplifier with a summing circuit for comparing voltages representing the actual and desired positions of the cylinder; 4) a servovalve driven by an electromagnetic torque motor; 5) hydraulic hoses connecting the ports of the cylinder with the ports of the servovalve; 6) a full-wave-phase, sensitive demodulator which receives the measurement LVDT signal; and 7) a frequency response analyzer which provides the sinusoidal test signal and analyzes the return signal to give frequency response data.

Three models of the fluid lines were compared with the experimental results. The dynamic response was defined in terms of the actual and desired positions of the piston. The simplest line model is obtained by assuming that the pressures and flows remain uniform all along the line. This

Received September 21, 1970.

* Assistant Professor of Engineering.
† Professor of Mechanical Engineering.